FWI without low frequency data - beat tone inversion

Wenyi Hu, Advanced Geophysical Technology Inc.*

Summary

Inspired by interference beat tone, a phenomenon commonly used by musicians for tuning check, we developed a novel full waveform inversion (FWI) method called beat inversion for reliable velocity model building without low frequency seismic data. In this new method, by utilizing two recorded seismic waves with slightly different frequencies propagating through subsurface, we are able to extract very low wavenumber (large scale structure) components from high frequency seismic data. With the conventional FWI algorithms, this type of long wavelength information can only be obtained by inverting low frequency seismic data. We designed and investigated two algorithms for this new method, one is the so-called amplitude-frequency differentiation (AFD) beat inversion, and the other is the phase-frequency differentiation (PFD) beat inversion. The AFD algorithm works for transmission seismic data with accurate amplitude measurement. The PFD is a more robust algorithm applicable for both transmission data and reflection data inversion and can be used for complex velocity model building applications. The mathematical analysis and the numerical experiment validate that this new FWI algorithm overcomes the long existing difficulty in FWI – the cycle-skipping issue. Another unique and important feature of the PFD beat inversion algorithm is that it does not require accurate source estimation and it is insensitive to amplitude measurement error. The numerical example shows that, with high frequency seismic data, the beat inversion method produces very smooth velocity model with large scale structural information properly recovered. On the other hand, if we invert the same frequency seismic data using the conventional FWI algorithm, many artifacts arising from cycle-skipping are observed and the inversion is trapped in local minima.

Introduction

Unlike traditional velocity model building tools using only kinematic information such as velocity tomography, full waveform inversion (FWI) utilizes full waveform information contained in seismic data to render high resolution velocity model through optimal data fitting.

One of the long existing difficulties we are facing in full waveform inversion is the cycle-skipping issue when low frequency seismic data are not available. Without low frequency seismic data and a good starting velocity model, both frequency domain and time domain full waveform inversion become very nonlinear and the iteration can be easily trapped in local minima thus produce a wrong velocity model. Therefore, many research efforts have been made to solve the cycle-skipping problem. The most straightforward strategy is the two-step velocity model building (Operto et al., 2004; Brenders and Pratt, 2007), where a traditional traveltime tomography is implemented first to obtain a smooth velocity model with proper kinematic information and then FWI is applied on this smooth model to further enhance the resolution and resolve fine structural features. A similar strategy, which is more automatic, is the combination of wave equation tomography and full waveform inversion (Symes, 2008; Biondi and Almomin, 2012). This method is more computationally expensive depending on specific implementation procedures. Shin and Cha (2008) proposed a full waveform inversion algorithm in the Laplace domain to recover large scale structures without low frequency data but this method is sensitive to signal-to-noise ratio and the accuracy of source estimation (Ha and Shin, 2012). To mitigating the cycle-skipping issue, Choi and Alkhalifah (2011) developed a frequency domain waveform inversion method with the phase unwrapping procedure to eliminate the phase ambiguity within the seismic data. However, phase unwrapping is not trivial, even for synthetic data. A more recent work addressing cycle-skipping issue was reported by Ma and Hale (2013), where reflection travel time inversion through dynamic warping technique is combined with FWI.

In this work, we developed a novel full waveform inversion algorithm for velocity model building without low frequency seismic data, using a strategy different from the work mentioned above. The main idea of our algorithm is that the interference between two propagating seismic waves at two slightly different high frequencies carries a great amount of low wavenumber (i.e., long wavelength) information. If we focus on this low wavenumber information and suppress the high wavenumber information with some techniques, then we are able to properly reconstruct the large scale structures in the earth model. The techniques we employed for high wavenumber suppression are similar to modulation and demodulation commonly used in signal processing community.

First, a simple amplitude-frequency differentiation (AFD) algorithm was developed based on amplitude modulation. This algorithm can be used for high quality transmission seismic data inversion. However, in complex velocity model building projects, seismic data include both transmission and reflection energy with significant measurement errors and source wavelet is usually unknown, then the AFD algorithm might not be applicable. For this reason, we developed another algorithm called phase-frequency differential (PFD) beat inversion, which is more robust and effective. The main feature of this algorithm is: 1) no cycle-skipping issue when low frequency data are not available; 2) accurate source estimation is not required; 3) computational expense is same as the conventional FWI algorithms; 4) insensitive to measurement error and noise.

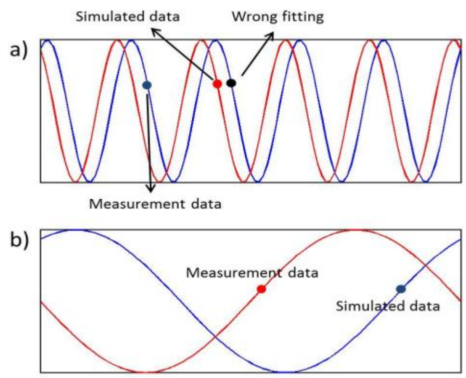

Figure 1: For same perturbation of medium property, a) cycle-skipping phenomenon is observed for high frequency case; b) no cycle-skipping for low frequency case.

Conventional FWI, Nonlinearity, and Cycle-skipping

The acoustic wave propagation equation can be written as:

$$\nabla^2 p + \omega^2 \rho\kappa p = -i\omega Q \qquad (1)$$

where p is the pressure, q is the volume density of mass acting as the source, and κ is the compressibility and we have the p wave velocity $v_p = 1/\sqrt{\rho\kappa}$.

The goal of full waveform inversion is, starting from a initial model κ_0, gradually updating the model by using the gradient information and eventually obtaining a model $\kappa_n = \kappa_0 + \Delta\kappa$ close to the true model κ_{true}, such that the simulated data $p(\omega,\kappa)$ fit the measurement data $p(\omega,\kappa_{true})$. The gradient information is calculated from the sensitivity kernel (i.e., the response of the simulated data to the perturbation of the medium property):

$$\partial p/\partial\kappa = -\rho\omega^2 \int_\tau p(\omega,\kappa;\mathbf{x},\mathbf{x_R}) G(\omega,\kappa;\mathbf{x},\mathbf{x_S}) d\mathbf{x}\,. \qquad (2)$$

Apparently, $\partial p/\partial\kappa$ is a function of κ, indicating that this is a nonlinear inversion problem and the level of nonlinearity depends on frequency. If the simulated data at $\kappa=\kappa_0$ and the measurement data at $\kappa=\kappa_{true}$ are out of phase for more than a half period, then the gradient-based search direction will be wrong due to cycle-skipping. Figure 1 shows a diagram of cycle-skipping phenomenon, where for the same amount of medium property perturbation, gradient-based search direction is wrong for high frequency case but for low frequency data there is no such problem.

Beat Tone

When two single frequency sounds have slightly different frequencies, the interference between these two sounds results in variations in volume. The volume variation rate is determined by the difference between the two sound frequencies. If the first signal $S_1=\cos(2\pi f_1 t)$, the second signal $S_2=\cos(2\pi f_2 t)$, $|f_1-f_2| << f_1$ and f_2, then we have the summation of these two signals:

$$S = S_1 + S_2 = 2\cos\left(2\pi\frac{f_1+f_2}{2}t\right)\cos\left(2\pi\frac{f_2-f_1}{2}t\right) \quad (3)$$

i.e., a low frequency signal modulated by a high frequency carrier signal, as shown in Figure 2. Demodulation procedure can remove the high frequency components and extract the low frequency components, the envelope, which is exactly what we need for full waveform inversion when no real low frequency seismic data are available.

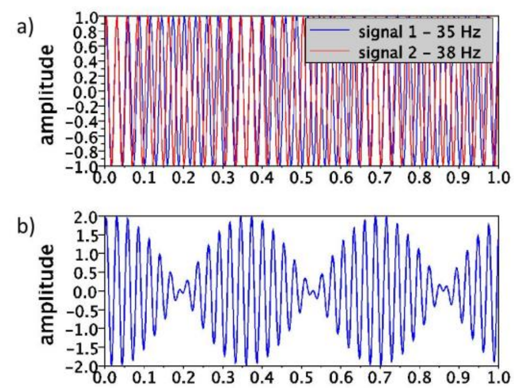

Figure 2: a) two single signals with slightly different frequencies (35 Hz and 38 Hz); b) the summation of the two signal produces a amplitude variation pattern and the varation rate is determined by the difference between the two frequencies.

Amplitude-Frequency Differentiation Beat Inversion

Observing Figure 2(b), we find that we can easily demodulate the signal by computing the envelope of the signal. This observation leads to the amplitude-frequency differentiation (AFD) inversion. A key point needs to be mentioned is that what we actually need for successful FWI is not low frequency components, but the low wavenumber components, although they are equivalent in the conventional FWI algorithms. The algorithms developed in this work were designed to extract low wavenumber information from high frequency data. Here we use a very simple example to show how to achieve this goal using AFD method. In this example, a source is located at (x=0, z=0) and the 313 receivers are deployed evenly (with interval of 12.5 m) from x=100 m to x=4000 m at same depth (z=0). The velocity is constant (v=2000 m/s). We recorded 3 sets of seismic data at the receivers (S_1 at f=15 Hz, S_2 at f=12 Hz, and S_3 at f=1.5 Hz). The real part of S_1 and S_2 are plotted in Figure 3(a), which contains relatively high wavenumber components because $k=\omega/v$. In Figure 3(b), the black curve is the absolute value of the real part of S_3 (i.e., f=1.5 Hz) while the blue curve is the amplitude (or envelope) of the summation of S_1 and S_2 (i.e., $|S_1+S_2|$). Figure 3(b) means that $|S_1+S_2|$ carries the same wavenumber information as the very low frequency data S_3. This is not surprising since

$$S_1+S_2=\frac{2}{|x|}\cos\left(\frac{k_1-k_2}{2}x\right)\exp\left(-i\frac{k_1+k_2}{2}x\right). \qquad (4)$$

If we invert $|S_1+S_2|$ instead of S_1 or S_2, large scale structures can be recovered without local minimum issue.

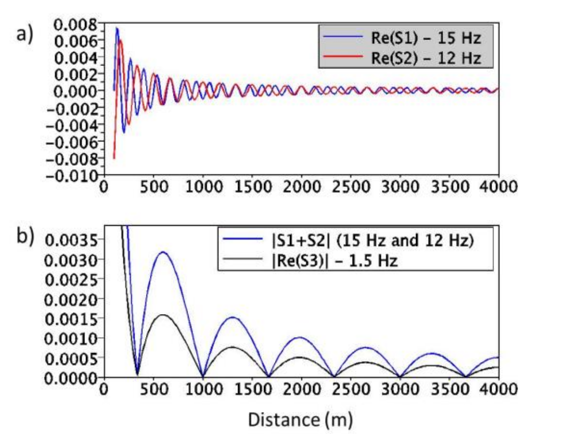

Figure 3: a) real part of s_1 (f =15 Hz) and s_2 (f = 12 Hz); b) absolute value of real part of very low frequency data s_3 (f = 1.5 Hz) and amplitude of s_1+s_2.

The cost function for AFD inversion algorithm is

$$C(\mathbf{m}_n)=\frac{1}{2}\left\| |S(\omega_1)+S(\omega_2)|^2-|M(\omega_1)+M(\omega_2)|^2\right\|^2 \qquad (5)$$
$$+\lambda_n R_n(\mathbf{m}_n)$$

where S is the simulated data and M is the measurement data, $\mathbf{m}$ is the unknowns to be inverted, $\boldsymbol{\lambda}$ is the regularization parameter, R is the regularization term, ω is the angular frequency ($|\omega_1-\omega_2|<<\omega_1$ and ω_2) the subscript n denotes the iteration index.

For field data, source estimation error, measurement error, reflection and scattered energy, and many other factors will have negative impact on amplitude demodulation performance and the high wavenumber components cannot be suppressed effectively. Therefore, we developed a more robust algorithm, the phase-frequency differentiation beat inversion algorithm (PFD).

Phase-Frequency Differentiation Beat Inversion

During seismic survey, different frequency components are recorded simultaneously and the interferences between different frequency components are naturally embedded in the recorded data causing the amplitude variations. This is the basis of AFD method (i.e., the default operation on different frequency components is summation). Actually, we can always extract single frequency components from the raw seismic data and apply any operation other than summation. In phase-frequency differentiation method (PFD), the summation operation is replaced by division to remove the effect of source estimation uncertainty, measurement error, unnecessary cross talk between reflection energy, etc. We use a simple layered velocity model shown in Figure 4 just for 1D scenario analysis.

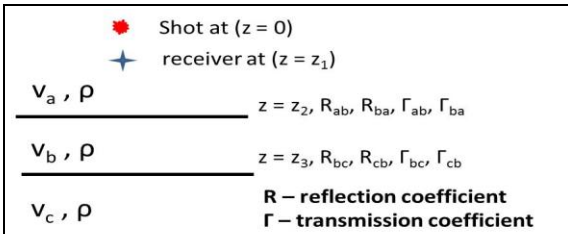

Figure 4: Diagram for 1D PFD reflection data analysis

Assuming that the 1D source amplitude is A and ignoring internal multiples, we have the reflection data S_R received at $z=z_1$ as

$$\begin{aligned} S_R(\omega) &= A\{R_{ab}+R_{bc}\Gamma_{ab}\Gamma_{ba}\exp[-ik_b(\omega)2(z_3-z_2)]\}\cdot \\ &\quad \exp[-ik_a(\omega)(2z_2-z_1)] \\ &= A\{B(\omega)\exp[-i\xi k_b(\omega)2(2(z_3-z_2))]\}\cdot \\ &\quad \exp[-ik_a(\omega)(2z_2-z_1)] \end{aligned} \qquad (6)$$

where B is a real number, and ξ, which will be discussed later, is a function of reflection coefficient R, transmission coefficient Γ, wavenumber k, and depth z.

Instead of inverting the reflection data S_R, in PFD algorithm, we invert the phase-frequency differentiation data defined as

$$\begin{aligned} \Phi\left[\frac{S_R(\omega_2)}{S_R(\omega_1)}\right] &= \Phi[\exp(-i\Delta k_a(2z_2-z_1))]+ \\ &\quad \Phi\{\exp[-i\xi\Delta k_b 2(z_3-z_2)]\} \end{aligned}, \qquad (7)$$

where Φ means phase. Because $\Delta k=k(\omega_2)-k(\omega_1)<<k(\omega_1)$, $k(\omega_2)$, $\xi(k_1)\approx\xi(k_2)=\xi$. An important condition needs to be emphasized here is that $2\Delta k_b(z_3-z_2)$ must be controlled within $(-\pi,\pi]$ through proper choice of ω_2 and ω_1. With this condition, we have $0<\xi\leq 1$ and the high wavenumbers k_a and k_b in (6) are replaced by low wavenumber Δk_a and $\xi\Delta k_b$. Consequently, the cycle-skipping issue is avoided. Otherwise, if this condition is not satisfied, then the phase ambiguity still exists in the phase-differentiation data. In practical implementation, this condition can be relaxed because the inversion algorithm usually converges as long as most data points do not have phase ambiguity issue.

The mechanism of PFD algorithm is similar to a phase demodulation technique. Due to this fact, this algorithm is insensitive to amplitude measurement error, the unknown attenuation parameter Q, and the uncertainty of mass density. In addition, source estimation is not required. Even the estimation of the source phase is not necessary. The information needs to be input into the inversion algorithm is the near field phase difference between the two frequencies, which can be obtained easily by analyzing the direct arrival data with short offsets.

The cost function for PFD inversion is

$$C(\mathbf{m}_n) = \frac{1}{2}\left\|\Phi\left[S(\omega_2)/S(\omega_1)\right] - \Phi\left[M(\omega_2)/M(\omega_1)\right]\right\|^2 + \lambda_n R_n(\mathbf{m}_n) \quad (8)$$

and the gradient of the cost function is derived as

$$\mathbf{g}(\mathbf{m}) = \mathrm{Im}\left(\frac{1}{\mathbf{S}(\omega_2)}\frac{\partial \mathbf{S}(\omega_2)}{\partial \mathbf{m}} - \frac{1}{\mathbf{S}(\omega_1)}\frac{\partial \mathbf{S}(\omega_1)}{\partial \mathbf{m}}\right)\cdot \mathbf{Res}(\mathbf{m}) + \lambda \frac{\partial R(\mathbf{m})}{\partial \mathbf{m}}, \quad (9)$$

where **Res(m)** is the residual.

Numerical Examples

Marmousi model was used for testing the PFD algorithm. The true model and the initial model are shown in Figure 5.

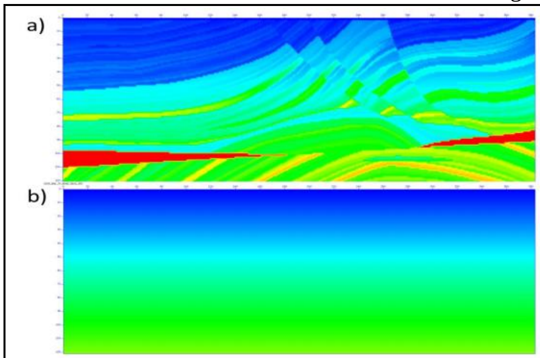

Figure 5: a) true Marmousi model; b) starting model

In this numerical experiment, the data at f_1 = 5 Hz and f_2 = 5.5 Hz are used for the PFD inversion and the result is shown in Figure 6(a). The result obtained by inverting 5 Hz data using the conventional FWI is shown in Figure 6(b), where many artifacts are observed because the gradient search direction in these areas are wrong due to the cycle-skipping phenomenon. We also note that the PFD inversion result has lower resolution than that obtained from the conventional FWI as expected.

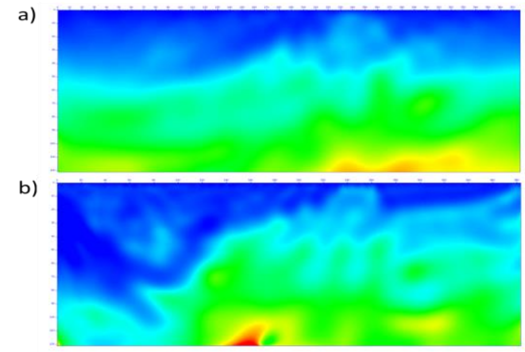

Figure 6: a) PFD inversion result using 5 Hz and 5.5 Hz data; b) conventional FWI inversion result using 5 Hz data.

Using the PFD inversion result shown in Figure 6(a) as the starting models, we implemented higher frequency FWI (5 Hz, 7.5 Hz and 12.5 Hz, 5 iterations for each frequency). The final results are shown in Figure 7.

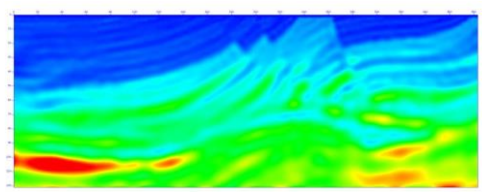

Figure 7: conventional FWI (5 Hz, 7.5 Hz, 12.5 Hz) using PFD (5 Hz, 5.5 Hz) inversion result as starting model.

Conclusions

We developed a novel full waveform inversion method for velocity model building without low frequency seismic data. Two algorithms were designed in this work referred to as the amplitude-frequency differentiation (AFD) method and phase-frequency differentiation (PFD). Instead of inverting the original seismic data directly, this new method inverts the interferences between two seismic data sets measured at slightly different frequencies. Through amplitude demodulation and phase demodulation, the new algorithms are able to extract low wavenumber components from high frequency seismic data to reconstruct large scale structures in the earth model, thus overcome the cycle-skipping issue. The numerical example validates that, without low frequency data, the PFD algorithm does not suffer from cycle-skipping phenomenon and produces a smooth velocity model with large scale structures recovered. On the other hand, inverting the same frequency seismic data, the conventional FWI algorithm yields a higher resolution model but with many artifacts and apparently be trapped in the local minimum.

References

Biondi, B. and A. Almomin, 2012, Tomographic full waveform inversion (TFWI) by combining full waveform inversion with wave-equation migration velocity anaylisis. SEG Technical Program Expanded Abstracts 2012: 1-5, doi: 10.1190/segam2012-0275.1.

Brenders, A. J. and R. G. Pratt, 2007, Efficient waveform tomography for lithospheric imaging: Implications for realistic 2D acquisition geometries and low frequency data: Geophysical Journal International, 168, 152–170, doi: 10.1111/gji.2007.168.issue-1.

Choi, Y. and T. Alkhalifah, 2011, Frequency-domain waveform inversion using the unwrapped phase. SEG Technical Program Expanded Abstracts 2011: 2576-2580, doi: 10.1190/1.3627727

Ha, W. and C. Shin, 2012, Laplace-domain full-waveform inversion of seismic data lacking low-frequency information: Geophysics, 77(5), R199–R206, doi: 10.1190/geo2011-0411.1.

Ma, Y. and D. Hale, 2013, Wave-equation reflection traveltime inversion with dynamic warping and hybrid waveform inversion, SEG Technical Program Expanded abstracts 2013, 871-876, doi: 10.1190/segam2013-0087.1

Operto, S., C. Ravaut, L. Improta, J. Virieux, A. Herrero, and P. Dell'Aversana, 2004, Quantitative imaging of complex structures from multi-fold wide aperture seismic data: A case study: Geophysical Prospecting, 52, 625–651, doi: 10.1111/gpr.2004.52.issue-6.

Shin, C., and Y. H. Cha, 2008, Waveform inversion in the Laplace domain: Geophysical Journal International, 173, 922–931, doi: 10.1111/gji.2008.173.issue-3.

Symes, W. W., 2008, Migration velocity analysis and waveform inversion: Geophysical Prospecting, 56, 765–790.